ELSEVIER

Journal of Molecular Catalysis A: Chemical 150 (1999) 37–47

JOURNAL OF MOLECULAR CATALYSIS A: CHEMICAL

www.elsevier.com/locate/molcata

Mechanism of oxygenative cleavage of catechols by nonheme iron complexes in relevance to catechol dioxygenases studied by quantum chemical calculations

Takuzo Funabiki *, Tamio Yamazaki

Department of Molecular Engineering, Graduate School of Engineering, Kyoto University, Sakyo-ku, Kyoto 606-8501, Japan

Received 2 February 1999; accepted 24 March 1999

Abstract

Mechanism of oxygenative cleavage of catechols by nonheme iron complexes was studied by quantum chemical calculations. Calculations based on the density-functional theory indicate that all carbon atoms of the DMC and Cat ligands of $[Fe^{III}(NH_3)_4(DMC)]^+$ (DMC: 3,5-dimethylcatecholate), $[Fe^{III}(NH_3)_4(Cat)]^+$ and $[Fe^{II}(NH_3)_4(Cat)]$ (Cat: catecholate) are positively charged, that is not favorable for the electrophilic attack. Significant amounts of the spin density, that are greater on oxygen than carbons, appear on the catecholate ligand. The spin density on aromatic carbon atoms is greater in the ferric complex than in the ferrous complex, supporting the Fe(II)-semiquinonate character of the ferric catecholate complexes. Results are obtained to support the probability of the initial binding of molecular oxygen to the iron center rather than to the aromatic carbons. In the step of the oxygen insertion into the C–C bond, formation of an epoxide-like structure is proposed. It is shown that the postulated intermediate can be converted to an oxygen-inserted product in the change of the electronic state from the anionic ligand to the neutral product.

Keywords: Catechol dioxygenase; Mechanism; Oxygen insertion process; Model catecholatoiron complexes; Quantum chemical calculation

1. Introduction

Catechol dioxygenases have been one of the most important enzymes in the development of bioinorganic chemistry and studied well from both sides of enzymes and models. Coordination environment around the iron center of ferric and ferrous enzymes has been studied by spectroscopic and crystallographic analyses [1,2]. As for the ferric enzymes that catalyze the intradiol cleavage of catechols, coordination of two histidines and two tyrosines [3–5] and one hydroxide [5] to the ferric center in protocatechuate 3,4-dioxygenase (3,4-PCD) has been indicated spectroscopically. This has been supported by the recent X-ray crystallographic analysis [6,7]. As for the ferrous enzymes that catalyze the extradiol cleavage of catechols, coordination of two histidines, one glutamate, and two waters has been indicated for biphenyl-cleaving Fe(II) dependent dioxygenase (BphC enzyme) by X-ray crystallography [8,9]. Two types of coordi-

* Corresponding author. Tel.: +81-75-753-5693; Fax: +81-75-753-5925; E-mail: funabiki@scl.kyoto-u.ac.jp

1381-1169/99/$ - see front matter
PII: S1381-1169(99)00198-3

nation of catechols have been suggested: a monodentate form in catechol 1,2-dioxygenase (1,2-CTD) [10] and a bidentate form in 3,4-PCD [5,11,12] and in BphC enzyme [8,9]. In case of 3,4-PCD, a five-coordination structure was indicated for the catecholate–iron species formed by replacement of one of tyrosine [6,7] rather than histidine [5] with a catecholate ligand.

Many model complexes have been reported for clarification of structure (structural models) and for clarification of reaction mechanisms and development of biomimetic oxygenation catalysis (functional models) [1,2]. The mechanism proposed on the basis of model chemistry, that seems mostly accepted so far, involves (1) an activation of a catecholate ligand for a direct reaction with molecular oxygen, (2) formation of a peroxy C–O–O–Fe species, and (3) transfer of an oxygen atom of the peroxo ligand between a C–C bond of the catecholate ligand to form a monooxygenated product (path A in Scheme 1). However, another path (path B in Scheme 1) which involves an initial oxygen binding to iron before formation of the peroxo species seems not to be excluded. In the proposed mechanisms, it is well accepted that activation of the coordinated catecholate ligand is important for the reaction with oxygen. Two types of activated carbon, i.e., radical [13–20] and anionic [21,22] carbons, have been proposed. The activated intermediate is represented, e.g., as a catecholatoiron(III) species with a radical character, but it may be probable in the model systems that a Fe(II)-semiquinonate species is in equilibrium with a Fe(III)-catecholate species. Recently, it is suggested that the mechanisms may be different between enzymatic and model systems [7]. This is because the product is formed from a six-coordinate species from model catecholate complexes [20,23–25] while the five-coordinate structure of the substrate-enzyme species is shown [7]. The formation of the extradiol oxygenation products from the five-coordinate catecholatoiron(III) complexes [8,9,26,27] has suggested importance of the open coordination site

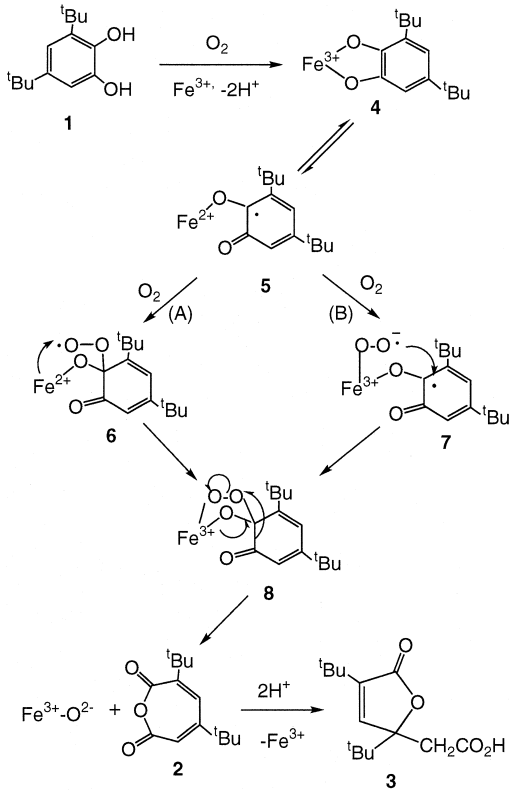

Scheme 1. Proposed mechanism of the oxygen insertion to the catecholate ligand.

for the extradiol oxygenations from not only Fe(II), but also Fe(III) species. Oxygenation of the six-coordinate model complex indicates that the five coordination environment seems not be essential for the intradiol oxygenation.

In the present study quantum chemical calculations have been performed on the model complexes to get further information about the oxygenation mechanism of catechol dioxygenases. Quantum chemical calculation studies are no doubt useful for getting insights on the mechanisms for which experimental information is not enough for clarification. However, systems involving iron and oxygen are one of the most difficult systems for calculations. The calculation method based on the density-functional theory is applied to iron systems under various simplifications of systems, e.g., with replacement of ligands by simple molecules [28–30] or without ligands [31] and changing oxidation

state of iron [32]. The aim of this paper is not to discuss in details or elaborate the calculation studies, but to give some probable ideas for problems unsolved in the oxygenation mechanism on the basis of the simplified calculations.

2. Experimental

Since the first model oxygenation was performed by the complexes coordinated by pyridine and bipyridine [14,15,33], efficient oxygenations by model complexes are favored by nitrogen-coordinating ligands, such as tris(2-pyridylmethyl)amine) (TPA) [19,20,23–25]. Thus, four nitrogen ligands (NH_3) are used here in place of chelating pyridine ligands for simplification. As substrated in the model reactions, 3,5-di-*tert*-butylcatechol ($DTBCH_2$, **1**), which is not a substrate for enzyme, is used extensively [1,2] while chlorocatechols, which are substrates for enzyme, are shown recently to be oxygenated catalytically [34]. **1** gives monooxygenated (**2**) and dioxygenated (**3**) products stepwise [15]. Here $[Fe(NH_3)_4(Cat)]^+$ and $[Fe(NH_3)_4(DMC)]^+$ are used for calculations by referring the structure of $[Fe(TPA)(DTBC)]^+$ which gives **2** and **3** under molecular oxygen [20].

Different calculation methods were used depending on the structures of molecules, and smaller basis sets were used in the more complicated systems. Calculations were performed for six-coordinate species, because formation of oxygenated species is experimentally demonstrated in the model systems and factors for calculation increase by the change of the coordination number from 6 to 5. In addition, the effect of distal amino acid residues which may play important roles in the enzymatic system is ignored in the present calculations.

2.1. Computer

Quantum chemical calculations were performed by using CRAY T94/4128 in Super-Computer Laboratory, Institute for Chemistry, Kyoto University.

2.2. Calculations for electronic states of $[Fe(NH_3)_4(DMC]^+$ (9), $Fe(NH_3)_4(Cat)]^+$ (10), and $[Fe(NH_3)_4(Cat)]$ (11)

Calculation method was based on the density-functional theory, using Gaussian 94 package with *BLYP* option as the exchange and correlation terms. Input file was prepared manually considering molecular symmetry. Atomic charges were calculated by the method of Mulliken population analysis. The ferric high-spin state and the +1 total charge were postulated for the complex. Structural parameters obtained for the complex $[Fe(TPA)(DTBC)](BPh_4)$ [23] by the X-ray crystallographic analysis were used as references for structures of model complexes **9** and **10** shown in Fig. 1. Point symmetric groups C_s and C_{2v} were postulated for **9** and **10**, respectively. MIDI-4 was used as a basis set [35]. Calculations were also performed for the Fe(II) complex (**11**) which has the 0 total charge in the aim to know the effect of the oxidation state of iron on the electronic state of the complex.

2.3. Calculations for the binding of molecular oxygen to the catecholatoiron complex

Two types of the insertion process of oxygen into the catecholate ligand were studied by using $[Fe(NH_3)_4(Cat)]^+$ as a model complex, depending on the direction of the approach of

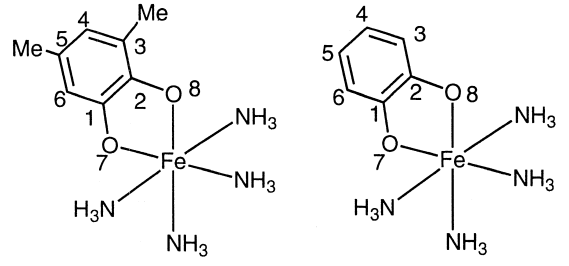

(**9**) [$Fe(NH_3)_4$ (DMC)]$^+$ (**10**) [$Fe(NH_3)_4(Cat)]^+$

Fig. 1. Model catecholatoiron complexes used for calculations.

oxygen to either the catecholate carbon atom or the iron center. Calculations were performed by a UHF method, using a relatively small basis set (3-21G) for convenience.

2.4. Calculations for probable structures of a catecholate–monooxygen adduct

Model calculations were performed for two probable structures of a catecholate–monooxygen adduct in a singlet state, with the total charge of either −2 or 0. Gaussian 94 program package, 6-31G basis set, and the RHF method were used in the calculations.

2.5. Model calculations for probable structures of a catecholate–Fe(O_2) ternary complex and the oxygen insertion process

Model calculations were performed for two probable structures of a catecholate–Fe(O_2) ternary complex in a quartet state, assuming the total charge as +1. Gaussian 94 program package, 6-31G basis set, and the UHF method were used in the calculations.

3. Results and discussion

*3.1. Electronic states of **9**, **10**, and **11***

Table 1 shows the atomic charge, the unpaired electron density, and the Frontier electron density (HOMO) of **9**. The results are mostly consistent with those obtained by the extended Hückel calculations [36]. The Mulliken population analysis indicates that the charge on the DMC ligand decreases from −2 to −0.82 and the spin density (0.86) appears on the ligand. On the other hand, the charge and the spin density on Fe are +1.38 and 3.91, respectively. Another characteristic result shown in Table 1 is that all carbon atoms of the DMC ligand are positively charged.

Table 1
Electron states of the catecholate ligand of [Fe(NH_3)$_4$(DMC)]$^+$ complex

Atom	Charge	Unpaired E.D.	Frontier E.D. (HOMO)
C1	+0.14	0.043	0.088
C2	+0.043	0.059	0.12
C3	+0.0017	0.023	0.024
C4	+0.037	0.056	0.075
C5	+0.076	0.049	0.082
C6	+0.035	0.026	0.0006
O7	−0.58	0.29	0.14
O8	−0.56	0.31	0.18
Fe	+1.38	3.91	0.023

E.D.: Electron density.

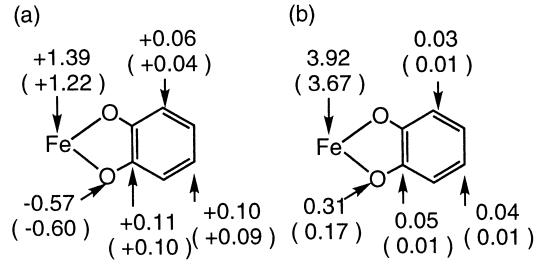

Fig. 2. (a) Atomic charge, (b) spin density of [$Fe^{III}(NH_3)_4Cat]^+$ (**10**) and [$Fe^{II}(NH_3)_4Cat$]) (**11**) (in parenthesis).

Effect of the oxidation state of iron on the electronic states of the complexes was studied by changing the total charge of the complexes, **10** and **11**, which have the spin multiplicity of 6 and 5, respectively. Results are shown in Fig. 2, in which data for **11** are shown in parenthesis. The atomic charges on the carbon atoms are not significantly different between **10** and **11**. On the other hand, the spin densities on the aromatic carbons are significant in the ferric complex, but not in the ferrous complex. The Mulliken atomic charge and the spin density on iron are also greater in the former than the latter, but differences were small.

Only qualitative discussions are allowed on the data shown in Table 1 and Fig. 2. Especially, atomic charges on iron should not be overestimated, because the method gives often the lower charges than those expected from the oxidation state. Qualitatively a little higher charge obtained for ferric than ferrous complexes reflects the difference of the total charge. However, it is difficult to claim on the values (+1.39 and +1.22) that the oxidation states of

not only ferrous but also ferric complexes are close to the high spin Fe(II). The relatively high atomic charges on the catecholate oxygen seem to be reasonable. The positive charges on all carbon atoms of the catecholate ligand conflict with the electrophilic attack by molecular oxygen to carbon atoms [7,22].

Although all spectroscopic results indicate that the iron of 3,4-PCD remains ferric throughout the reaction cycle, a Fe(II)-semiquinone complex is considered to be a reasonable active complex in the model systems [7]. The spin density appears not only on oxygen, but also on aromatic carbon atoms. This supports the contribution of the Fe(II)-semiquinonate structure on the oxygenation. Total amount of the spin density is higher in the ferric complex than ferrous, reflecting the greater electron transfer from the catecholate ligand to the ferric center than ferrous. Supposed the mechanism in which oxygen attacks homolytically the radical centers of the semiquinonate ligand, the spin density localized in the perpendicular orbital suggests that oxygen favors to approach the carbon atom from the perpendicular side against the aromatic ring plane rather than from the vertical side. In this case, oxygen attacks preferably C1 or C2 rather than C3 or C6, because the spin density and Frontier electron density (HOMO) are greater in the former. However, the spin densities on the carbon atoms are relatively very low in comparison with that on the oxygen atom, suggesting that the radical character of the carbon atoms is not so high as to support strongly the direct attack by oxygen to the carbon atoms.

On the other hand, the results in Table 1 and Fig. 2 suggest that the initial attachment of molecular oxygen to iron is probable even in Fe(III) as well as Fe(II) complexes. As shown by examples of Co(III)–R complexes which reactivity is explained by Co(II)–(·R) (R = H, alkyl, aryl) [37–42], it is probable that Fe(III)–catecholate complexes react as Fe(II)–semiquinonate complexes with oxygen. Magnetic susceptibility study on Fe(III)–catecholate complexes indicates the Fe(II)–semiquinonate character is greatly dependent on the substituent on the ligand [43]. The interaction between metal and dioxolane ligands (e.g., catecholate and semiqunonate ligands) has been studied with various metal complexes [44]. An interesting example is found in manganese complexes in which any significant π-bonding between manganese and the DTBSQ radical anion is absent [45,46] and electronic delocalization within the manganese-dioxolane chelate ring is very little [47].

3.2. Binding process of oxygen to the catecholatoiron complex

In the calculations for oxygen metal complexes, selection of spin-multiplicity is not unequivocal. In the present case, calculations were performed by assuming a high spin quartet state for all Fe/O_2 complexes. In the four possible states ($S = 7/2,\ 5/2,\ 3/2,\ 1/2$) caused by Fe(III) ($S = 5/2$) and O_2 ($S = 1$), $S = 7/2$ and $1/2$ are less probable for the high spin $Fe(III)/O_2$ system. Supposing that O_2 is in the triplet state in the initial approach to iron, it seems more probable that O_2 interacts with iron in the $S = 3/2$ state rather than $5/2$. This enables us to perform calculations by assuming only a quartet state for iron complexes throughout the reaction.

3.2.1. Oxygen attack to the catecholate carbon atom

In the calculation study on **10**, it was found that HOMO of α-electron is represented by **12** for **10** in Fig. 3. In the process of the direct interaction of molecular oxygen with a catecholate ligand (path A in Scheme 1), the interaction between SOMO of O_2 and SOMO of **10** (HOMO of α-electron) is thought to be important. This interaction takes place between the anti π^*-orbital of SOMO of O_2 and the anti π-orbital of the C–O bond of the catecholate ligand shown by **12**, leading the O_2 approach from the direction perpendicular to the aromatic

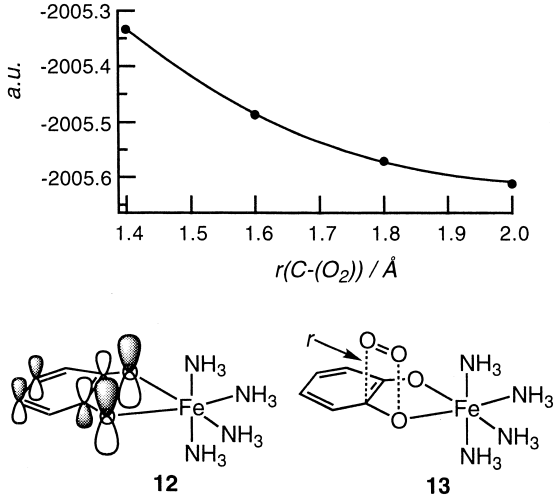

Fig. 3. Total energy change caused by the oxygen approach to a catecholate ligand.

plane and parallel to the C–O bond as shown by **13** in Fig. 3. Calculations were performed at the $C–O_2$ distance (r) shorter than 2 Å, because the complex may not be stabilized at the longer distance. As shown in Fig. 3, the total energy increases monotonously with the decreasing $C–O_2$ distance. There is no tendency to show a minimum point in the total energy curve. This suggests that the postulated process is not necessarily so favorable as expected from proposed mechanisms.

3.2.2. Oxygen coordination to iron

Another possible way of the O_2 attachment is the initial approach to the iron center as shown by the path B in Scheme 1. Though this process is not generally accepted in comparison with the path A, it is worthwhile to study the process by calculations. The binding of O_2 to Fe requires an open coordination site. A probable model may be derived from **10** by removing one NH_3 ligand, but this increases factors that should be considered in calculations. Since the oxygenation products are formed from the tetradentate TPA complexes such as $[Fe(TPA)(DTBC)]^+$ [20], the calculation study was performed here with another model complex, which was derived from **10** by changing the chelate catecholate ligand to the monodentate form with maintaining four NH_3 ligands. The model complex (**14**, Fig. 4) was derived from **10** by cutting a Fe–O1 bond and turning the catecholate ligand 90 degree around the C2–O bond. The total energy change was calculated by changing the $Fe–O_2$ bond length with the fixed bond angle $\angle Fe–O–O = 130°$. Considering that the $Fe–O_2$ bond distance is longer than the C–O bond, calculations were performed between 1.8 and 2.6 Å. As shown in Fig. 4, the total energy becomes minimum at Fe–O = ca. 2.0 Å, indicating that the complex can be stabilized by the coordination of oxygen. This result parallels the fact that the most Fe–O bonds of Fe–(O2) species are around 1.75–2.0 Å. The $Fe–(O_2)$ complex, if formed, may be very unstable since the complex is destabilized by the change of the catecholate coordination from chelate to monodentate.

3.3. Insertion of a peroxy oxygen atom into the C–C bond

Mechanistic studies on the catechol dioxygenases and model systems have suggested that

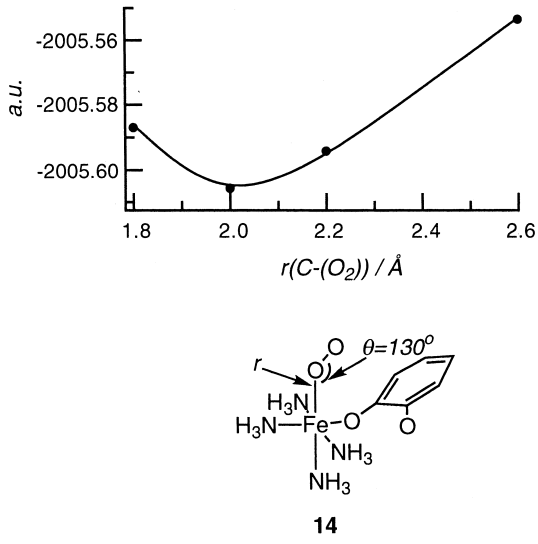

Fig. 4. Total energy change caused by the oxygen approach to an iron center.

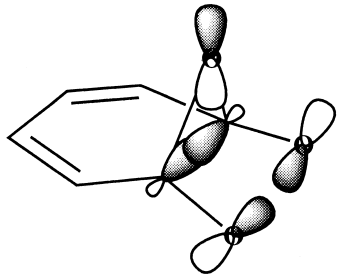

23

Fig. 5. HOMO of **21**.

oxygen is inserted to a catecholate ligand stepwise via a Fe–O–O–C species [1,2,6,15,20]. No direct evidence for formation of this type of peroxy iron species has been obtained, but it is thought that the isolation of analogous stable complexes which involve an M–O–O–C bond (M = Rh and Ir) gives a strong support for the Fe–O–O–C species [48,49]. The insertion process is explained by the Criegee rearrangement that is originally applied for organic hydroperoxide or alkyl peroxy esters. The Criegee rearrangement may proceed mostly by an intramolecular ionic reaction via either a bicyclic, highly oriented transition state or a tightly oriented intimate ion pair, though the rearrangement with homolytic decomposition has also been proposed in the case of *t*-alkyl peroxy esters [50]. The rearrangement has not been studied in detail when it is applied to peroxy iron species.

In the present study, model calculations were performed for the reaction in Eq. (1) to know how one of the oxygen atoms is inserted into the C–C bond of the catecholate ligand from the Fe–O–O–C species. Since the process is very complicated for calculations, calculations of only the part of the catecholate ligand was first tried, neglecting the iron part of the complex. This is connected with the oxygenative cleavage of catechol by the action of activated oxygen, e.g., superoxide ion and hydrogen peroxide, in the absence of assistance of metals [1]. The result was then tested to the iron complex by performing preliminary calculations.

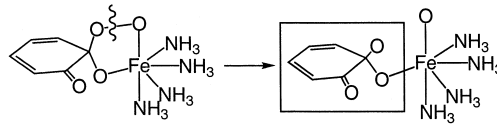

15 **16** (1)

3.3.1. Probable structures of the catecholate-monooxygen adduct

Two assumption was made for formation of a catecholate–monooxygen adduct and for insertion of an oxygen atom into the C–C bond: (1) the cleavage of the O–O bond may occur simultaneously with the formation of the C–O bond, but not necessarily with the insertion of the oxygen atom into the C–C bond, (2) the oxygen insertion into the C–C bond may promote the simultaneous dissociation of the product from iron, in which process the anionic catecholate ligand is converted to a neutral product. Thus, calculations were performed to know whether an oxygen atom attached to anionic organic species is inserted by the change of the total charge from −2 to 0.

Two structures, **17** in Eq. (2) and **20** in Eq. (3), were postulated as the structures before insertion of an oxygen atom. These structures

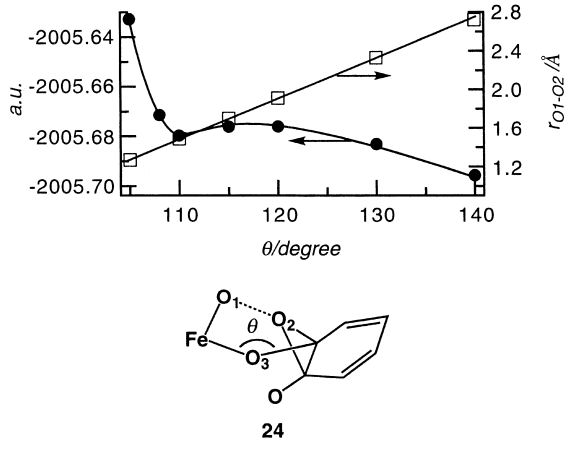

24

Fig. 6. Effect of θ on the total energy and the O–O distance.

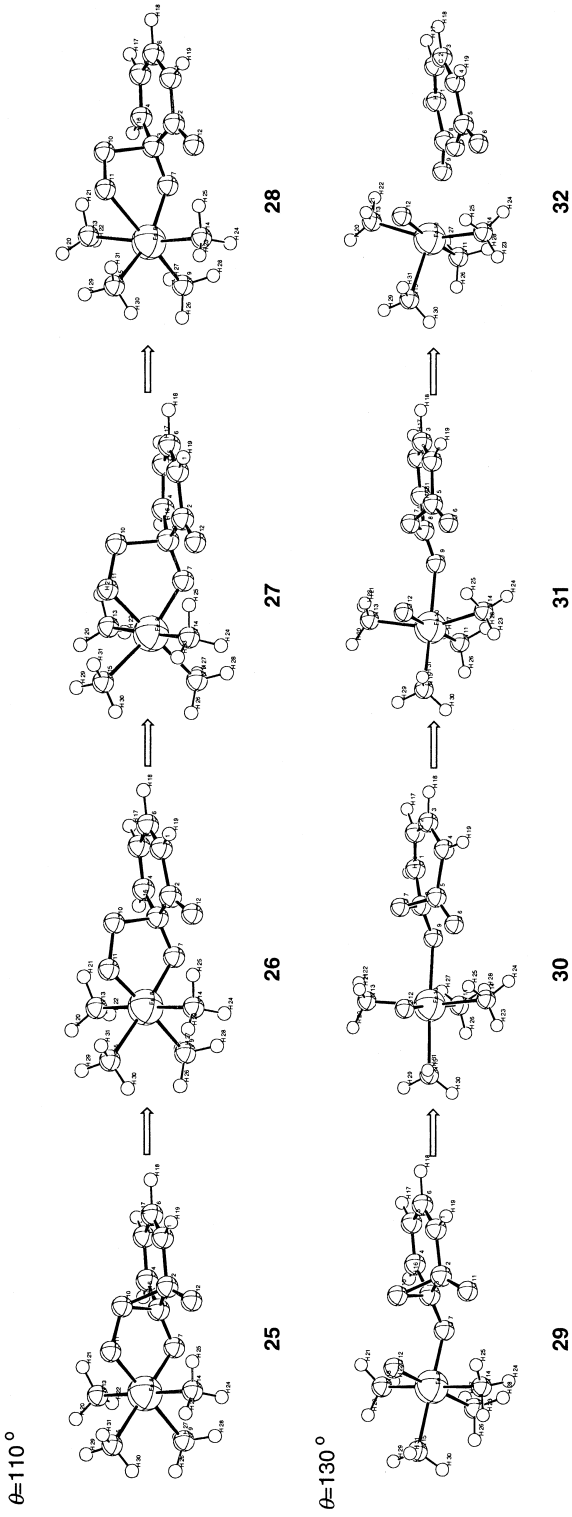

Fig. 7. ORTEP description of the oxygen intradiol insertion process.

are geometrically close to those proposed for transition states in the Criegee rearrangement [50]. The most stable anionic forms (total charge = −2) derived from **17** and **20** by optimization are **18** and **21**, respectively. **21** is 3.75 kcal/mol less unstable than **18**, suggesting that **21** is a structure closer to the transition state than **18**. The estimated C1–C2 bond distance (1.52 Å) in **21** indicates no bond breaking at this stage. An optimized neutral form derived from **18** by the change of the charge from −2 to 0 is **19**, in which the O–C–O bond angle becomes a little smaller than in **18**.

On the other hand, **21** is converted to the oxygen-inserted product **22** by the same procedure. The conversion of **21** to **22** is the 146.6 kcal/mol exothermic reaction, indicating that the reaction proceeds irreversibly. The driving force for the insertion of oxygen from **21** may be related to HOMO of **21** that is shown by **23** in Fig. 5. The orbitals between C1 and C2 are bonding and those between O and C1–C2 are antibonding. The change of the total charge of **21** from −2 to 0 removes electron from HOMO and contributes to weaken both the C1–C2 bonding and the anti-bonding between O and C1–C2, that promotes the insertion of oxygen. In this connection, it is interesting to know that one of the peroxo oxygen in the rhodium and iridium complexes is not fixed to the C2 carbon but interacts with both C1 and C2 [48,49].

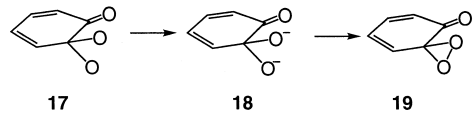

(2)

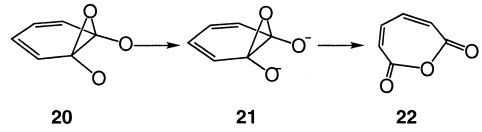

(3)

3.3.2. Probable structures of a catecholate-Fe(O_2) ternary complex for oxygen insertion

Since the model calculations described above suggest that the oxygen-inserted product **22** is derived from the epoxide type adduct **21**, calculations for a catecholate-Fe(O_2) ternary complex were tried with the model complex $[Fe(NH_3)_4(Cat)(O_2)]^+$. As shown in Fig. 6, Fe, O1, O2, and O3 are placed in the same plane in the model structure **24**. Since the structure-optimization computation for the iron containing model complexes was extremely slow in the

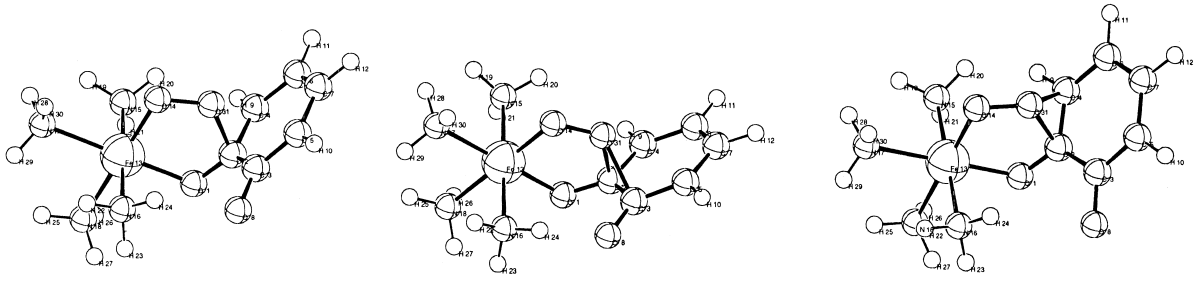

33 **34** **35**

Fig. 8. ORTEP description of the oxygen adduct for monodentate ligand.

present calculation process, it has not been successful in finding the optimized structures which are in the thermodynamically stabilized form. In addition, the more elaborate calculations are required for detailed discussions, considering the electronic correlation on the basis of the lower approximation. However, it is worthwhile to show the structural changes towards optimized structures and forces causing that change at the present stage.

The O–O bond fission and the total energy change were studied by changing the θ value between 105 and 140° in **24**. Fig. 6 shows the changes of the total energy and the O1–O2 bond distance caused by the change of θ. The total energy becomes minimum near at $\theta = 110°$ ($r_{(O1-O2)} = 1.49$ Å) and maximum near at $\theta = 120°$ ($r_{(O1-O2)} = 1.91$ Å). This suggests that the state near $\theta = 120°$ is close to the transition state for the O–O bond fission.

Fig. 7 shows ORTEP figures obtained in the structure-optimizing calculations performed at $\theta = 110$ and $\theta = 130°$. At $\theta = 110°$, structure **25** changes towards **28** (peroxo complex) by the force to separate the epoxide oxygen from the aromatic carbon. At $\theta = 130°$, structure **29** changes towards **32** with insertion of oxygen between the C1–C2 bond by the force to move the epoxide oxygen between C1 and C2 bond.

The calculation study has not been performed for the extradiol oxygenations. Chelate catecholate adducts have been isolated in the extradiol oxygenases and analyzed X-ray crystallographically [8,9,26,27]. However, the proposed mechanisms involve a monodentate species in the reaction of extradiol oxygenases [51–53]. This is consistent with that the epoxide-type oxygen adduct between C1 and C6 cannot be formed in the chelate complex for the steric reason, but only in the monodentate catecholate complex. As shown in Fig. 8, once a peroxo complex is formed with the monodentate ligand, **33**, it can be converted sterically to either intradiol or extradiol epoxide-type form (**34** or **35**). The probability of this process on the energetic base should be studied in the future.

Acknowledgements

We thank the Ministry of Education, Science, and Culture for Grants (No. 07455322, 07305062, 0215239, and 0216238), and Dr. S. Takenaka of Kyoto University and Prof. H. Kobayashi of Kurashiki University of Science and the Arts for discussions.

References

[1] T. Funabiki, Oxygenases and model systems, in: R. Ugo, B.R. James (Eds.), Catalysis by Metal Complexes, Vol. 19, Kluwer Academic Publishers, Dordrecht, 1997, pp. 1–393.
[2] L. Que Jr., R.Y.N. Ho, Chem. Rev. 96 (1996) 2607.
[3] L. Que Jr., J.D. Lipscomb, R. Zimmermann, E. Münck, N.R. Orme-Johnson, W.H. Orme-Johnson, Biochim. Biophys. Acta 452 (1976) 320.
[4] R.H. Felton, W.L. Barrow, S.W. May, A.L. Sowell, S. Goel, B.G. Stern, E.A. Stern, J. Am. Chem. Soc. 104 (1982) 6132.
[5] A.E. True, A.M. Orville, I.L. Pearce, J.D. Lipscomb, L. Que Jr., Biochemistry 29 (1990) 10847.
[6] D.H. Ohlendorf, A.M. Orville, J.D. Lipscomb, J. Mol. Biol. 244 (1994) 586.
[7] A.M. Orville, J.D. Lipscomb, D.H. Ohlendorf, Biochemistry 36 (1997) 10052.
[8] S. Han, L.D. Eltis, K.J. Timmis, S.W. Muchmore, J.T. Bolin, Science 270 (1995) 976.
[9] T. Senda, K. Sugiyama, H. Narita, T. Yamamoto, K. Kimbara, M. Fukuda, M. Sato, K. Yano, Y. Mitsui, J. Mol. Biol. 255 (1996) 735.
[10] L. Que Jr., R.B. Lauffer, J.B. Lynch, B.P. Bruce, J.W. Pyrz, J. Am. Chem. Soc. 109 (1987) 5381.
[11] A.M. Orville, J.D. Lipscomb, J. Biol. Chem. 264 (1989) 8791.
[12] R.B. Lauffer, L. Que Jr., J. Am. Chem. Soc. 104 (1982) 7324.
[13] T. Nakazawa, Y. Kojima, H. Fujisawa, M. Nozaki, O. Hayaishi, T. Yamano, J. Biol. Chem. 240 (1965) PC3224.
[14] T. Funabiki, A. Mizoguchi, T. Sugimoto, S. Yoshida, Chem. Lett. (1983) 917.
[15] T. Funabiki, A. Mizoguchi, T. Sugimoto, S. Tada, M. Tsuji, H. Sakamoto, S. Yoshida, J. Am. Chem. Soc. 108 (1986) 2921.
[16] T. Funabiki, T. Konishi, S. Kobayashi, A. Mizoguchi, M. Takano, S. Yoshida, Chem. Lett. (1987) 719.
[17] T. Funabiki, S. Tada, T. Yoshioka, M. Takano, S. Yoshida, J. Chem. Soc., Chem. Commun. (1986) 1699.
[18] T. Funabiki, H. Kojima, M. Kaneko, T. Inoue, T. Yoshioka, T. Tanaka, S. Yoshida, Chem. Lett. (1991) 2143.
[19] D.D. Cox, S.J. Benkovic, L.M. Bloom, F.C. Bradley, P.J. Nelson, L. Que Jr., D.E. Wallick, J. Am. Chem. Soc. 110 (1988) 2026.
[20] D.D. Cox, L. Que Jr., J. Am. Chem. Soc. 110 (1988) 8085.

[21] L. Que Jr., Coord. Chem. Rev. 50 (1983) 73.
[22] S. Fujii, H. Ohya-Nishiguchi, N. Hirota, A. Nishinaga, Bull. Chem. Soc. Jpn. 66 (1993) 1408.
[23] H.G. Jang, D.D. Cox, L. Que Jr., J. Am. Chem. Soc. 113 (1991) 9200.
[24] W.O. Koch, H.-J. Krüger, Angew. Chem., Int. Ed. Engl. 34 (1995) 2671.
[25] M. Duda, M. Pascaly, B. Krebs, J. Chem. Soc. Chem. Commun. (1997) 835.
[26] M. Ito, L. Que Jr., Angew. Chem., Int. Ed. Engl. 36 (1997) 1342.
[27] T. Ogihara, S. Hikichi, M. Akita, Y. Moro-oka, Inorg. Chem. 37 (1998) 2614.
[28] K. Yoshizawa, J. Biol. Chem. 3 (1998) 318.
[29] K. Yoshizawa, Y. Shiota, T. Yamabe, Chem. Eur. J. 3 (1997) 1160.
[30] K. Yoshizawa, T. Ohta, T. Yamabe, R. Hoffmann, J. Am. Chem. Soc. 119 (1997) 12311.
[31] L. Andrews, G.V. Chertihin, A. Ricca, C.W. Baushlicher Jr., J. Am. Chem. Soc. 118 (1996) 467.
[32] L. Öhrström, I. Michaud-Soret, J. Am. Chem. Soc. 118 (1996) 3283.
[33] T. Funabiki, H. Sakamoto, S. Yoshida, K. Tarama, J. Chem. Soc. Chem. Commun. (1979) 754.
[34] T. Funabiki, T. Yamazaki, A. Fukui, T. Tanaka, S. Yoshida, Angew. Chem., Int. Ed. Engl. 37 (1998) 513.
[35] J. Andzelm, S. Huzinaga, M. Klobukowski, E. Radzio-Andzelm, Y. Sakai, H. Tatewaki, Gaussian basis sets for molecular calculations, in: S. Huzinaga (Ed.), Physical Sciences Data, Vol. 16, Elsevier, Amsterdam, 1985.
[36] T. Funabiki, T. Inoue, H. Kojima, T. Konishi, T. Tanaka, S. Yoshida, J. Mol. Catal. 59 (1990) 367.
[37] T. Funabiki, M. Matsumoto, K. Tarama, Bull. Chem. Soc. Jpn. 45 (1972) 2723.
[38] T. Funabiki, K. Tarama, Bull. Chem. Soc. Jpn. 45 (1972) 2945.
[39] T. Funabiki, M. Mohri, K. Tarama, J. Chem. Soc. Dalton Trans. (1973) 1813.
[40] B.D. Gupta, T. Funabiki, M.D. Johnson, J. Am. Chem. Soc. 98 (1976) 6697.
[41] T. Funabiki, B.D. Gupta, M.D. Johnson, J. Chem. Soc. Chem. Commun. (1977) 653.
[42] A. Bury, C.J. Cooksey, T. Funabiki, B.D. Gupta, M.D. Johnson, J. Chem. Soc. Perkin Trans. II (1979) 1050.
[43] T. Funabiki, A. Fukui, To be submitted.
[44] C.G. Pierpont, C.W. Lange, Prog. Inorg. Chem. 41 (1994) 331.
[45] T. van der Graaf, D.J. Stufknes, J. Vichova, A. Vlcek Jr., J. Organomet. Chem. 401 (1991) 305.
[46] F. Hartl, D.J. Stufkens, A. Vlcek Jr., Inorg. Chem. 31 (1992) 1687.
[47] F. Hartl, A. Vlecek Jr., Inorg. Chem. 35 (1996) 1257.
[48] P. Barbaro, C. Bianchini, C. Mealli, A. Meli, J. Am. Chem. Soc. 113 (1991) 3181.
[49] P. Barbaro, C. Bianchini, P. Frediani, A. Meli, F. Vizza, Inorg. Chem. 31 (1992) 1523.
[50] B. Plesnicar, Organic polyoxides, in: S. Patai (Ed.), The Chemistry of Peroxides, Vol. 483, Wiley, Chichester, 1983.
[51] A.M. Orville, J.D. Lipscomb, J. Biol. Chem. 268 (1993) 8596.
[52] P.A. Mabrouk, A.M. Orville, J.D. Lipscomb, E.I. Solomon, J. Am. Chem. Soc. 113 (1991) 4053.
[53] L. Shu, Y.-M. Chiou, A.M. Orville, M.A. Miller, J.D. Lipscomb, L. Que Jr., Biochemistry 34 (1995) 6649.